

Early dynamical instabilities in the giant planet systems

E. Lega,¹* A. Morbidelli¹ and D. Nesvorný²

¹Université de Nice Sophia Antipolis, CNRS UMR 7293, Observatoire de la Côte d'Azur, Bv. de l'Observatoire, BP 4229, F-06304 Nice cedex 4, France

²Southwest Research Institute, Department of Space Studies, 1050 Walnut St, Suite 300, Boulder, CO 80302, USA

Accepted 2013 March 6. Received 2013 March 4; in original form 2013 January 28

ABSTRACT

The observed wide eccentricity distribution of extrasolar giant planets is thought to be the result of dynamical instabilities and gravitational scattering among planets. Previously, it has been assumed that the orbits in giant planet systems become gravitationally unstable after the gas nebula dispersal. It was not well understood, however, how these unstable conditions were established in the first place.

In this work, we numerically simulate the evolution of systems of three planets as the planets sequentially grow to Jupiter's mass, and dynamically interact among themselves and with the gas disk. We use the hydrodynamical code *FARGO* that we modified by implementing the *N*-body integrator *SYMBA*. The new code can handle close encounters and collisions between planets. To test their stability, the planetary systems were followed with *SYMBA* for up to 10^8 yr after the gas disc dispersal.

We find that dynamics of the growing planets is complex, because migration and resonances raise their orbital eccentricities, and cause dynamical instabilities when gas is still around. If the dynamical instabilities occur early, planets can be removed by collisions and ejections, and the system rearranges into a new, more stable configuration. In this case, the planetary systems emerging from the gas discs are expected to be stable, and would need to be destabilized by other means (low-mass planets, planetesimal discs, etc.). Alternatively, for the giant planet system to be intrinsically unstable upon the gas disc dispersal, a special timing would be required with the growth of (at least some of) the giant planets having to occur near the end of the gas disc lifetime.

Key words: Planet–disc interactions.

1 INTRODUCTION

The eccentricity distribution of the extrasolar giant planets is wide with orbits commonly having $e > 0.3$. Such a wide distribution was unexpected based on our anticipation from the Solar system planets. Different mechanisms have been proposed to explain the high-eccentricity values: trapping of planetary pairs in mean motion resonances (Lee & Peale 2002), the Kozai cycles in binary systems (Holman, Touma & Tremaine 1997; Mazeh, Krymolowsky & Rosenfeld 1997), stellar jets (Namouni 2005) and gravitational scattering during global dynamical instabilities (Rasio & Ford 1996; Weidenshilling & Marzari 1996; Lin & Ida 1997).

This last mechanism has been investigated with extensive *N*-body simulations (Chatterjee et al. 2008; Juric & Tremaine 2008; Raymond et al. 2009). All these studies assumed that the planetary systems emerging from the gas discs are intrinsically unstable, and the gravitational interactions among planets cause instabilities

after the gas disc dispersal. The subsequent scattering encounters between planets lead to large orbital eccentricities, just as needed to explain the observations.

A hydrodynamical code has been recently used to study the planetary system instabilities in a low-density rapidly dispersing disc (Moeckel & Armitage 2012). The initial orbits of the planets were assumed to be circular and close enough to each other to be unstable, without any mutual resonance relationship. It was found that the disc can stabilize some of the planetary systems by driving them into resonance rapidly. However, the systems that became unstable ended up behaving as in the gas-free simulations.

The investigations discussed above, including Moeckel & Armitage (2012), adopt similar choices of initial conditions with unstable and sometimes overlapping planetary orbits. In reality, the initial conditions of these studies should be informed from the previous stages of planet–disc interactions when the damping effects of gas were important.

The orbital dynamics of giant planets in a massive gas disc has been studied with a hydrodynamical code by Marzari, Baruteau & Scholl (2010). They started their simulations with the fully formed

* E-mail: elena@oca.eu

giant planets and ignored the previous stage during which the giant planets had grown by gas accretion on to their cores.

Here, we report the result of the first effort to investigate the dynamical evolution of planets from their growth phase from cores to aftermath of the gas disc dispersal. Our simulation set-up is different from those of previous works and is defined according to the following rationale. Planetary cores are expected to form by oligarchic growth (Kokubo & Ida 1998) with orbital separations of about 10 mutual Hill radii. However, during and after their formation they migrate in the disc due to their gravitational interactions with the gas. According to the Pollack et al. model (Pollack et al. 1996), the cores can spend a few millions years in the disc before accreting gas in a runaway fashion and become giant planets. In this time they can substantially modify their orbits and reach a new equilibrium configuration. While it was thought in the past that cores continuously migrate towards the central star (Ward 1997), it is now known that in a disc with realistic heat diffusion they migrate towards an orbital radius where migration is cancelled (Paardekooper & Mellema 2006; Kley, Bitsch & Klahr 2009; Lyra, Paardekooper & Mac Low 2010). This no-migration radius acts as a *planet trap*. If multiple cores are present, they are expected to reach a resonant non-migrating configuration near the trap (Morbidelli et al. 2008). In this configuration, the cores can be much closer to each other than their initial 10 Hill radii separation which may lead to very strong instabilities when the planets grow to Jupiter mass.

With this kind of dynamical evolution in mind, in our hydrodynamical simulations we set up a planet trap and let a system of three embryos of $10 M_{\oplus}$ to evolve until they reach a stable resonant configuration. Then, we track the evolution of the systems as each of the three planets grows in sequence to one Jupiter mass. Finally, we slowly remove the gas from the disc and follow the evolution of the systems up to 10^8 yr after the gas dispersal. We use the hydrodynamical code `FARGO` (Masset 2000) modified in Morbidelli & Nesvorny (2012) by implementing the N -body integrator `SYMBA` (Duncan, Levison & Lee 1998)¹ to handle close encounters and mutual collisions between planets.

The paper is organized as follows. Section 2 explains the set-up of our numerical simulations. The dynamics of growing planets is described in Section 3. We then discuss the effects of the gas disc dispersal and the subsequent stage of purely N -body interaction of the remaining planets (Section 4). Conclusions are given in Section 5.

2 SET-UP OF NUMERICAL SIMULATIONS

2.1 Disc parameters

We used the hydrodynamical two-dimensional code `FARGO` (Masset 2000), in which the original N -body Runge–Kutta integrator was replaced (Morbidelli & Nesvorny 2012) with the symplectic integrator `SYMBA` (Duncan et al. 1998). The `SYMBA` code was specifically designed to handle close encounters and mutual collisions between planets. As the hydrodynamical simulations are CPU expensive, we were not able to run many simulations to fully explore parameter space. Instead, we considered a few cases that illustrate different aspects of the problem.

Two different discs were considered (denoted by A and B in the following) with the initial mass $M_A = 0.009 M_{\odot}$ in case A and $M_B = 0.018 M_{\odot}$ in case B , where M_{\odot} is the mass of the Sun. In

each case, we performed several simulations that differed in the prescription for the growth of the planets (see below).

We use units such that $G = 1$ and $M_{\odot} = 1$. The orbital period of a planet with semimajor axis $a = 1$ is therefore $T = 2\pi$. We normalize the time t by T in the following, so that t corresponds to the number of orbits at $a = 1$, or years. The disc’s kinematic viscosity coefficient is set to be $\nu = 10^{-5}$ in these units. The initial surface density profile scales with the distance r from the star as $r^{(-1/2)}$.

Our computational domain consists of an annulus of the protoplanetary disc extending from r_{\min} to r_{\max} . Different disc extensions have been used in different cases. In some cases (specified below), the disc had to be extended during the simulations when the migration caused the innermost planet to approach the inner boundary. To start with, we used $r_{\min} = 0.5$, $r_{\max} = 4.5$, and a grid of $N_r = 660$ linearly spaced radial cells and $N_s = 700$ azimuthal cells.

The width of planet’s horseshoe region is given, in the isothermal disc approximation (Masset, D’Angelo & Kley 2006b), by

$$x = \sqrt{\frac{(m/M_{\odot})}{(H/r)}} a. \quad (1)$$

For example, for a planet of mass $m/M_{\odot} = 3 \times 10^{-5}$ (i.e. $10 M_{\oplus}$) and disc aspect-ratio $H/r = 0.05$, we get $x = 0.0245a$, where a is the semimajor axis (see Section 2.2). The radial resolution of 0.006 allows us to resolve the horseshoe region by at least four cells for any $a \geq 1$.

The planetary contribution to the potential Φ acting on the disc is smoothed according to

$$\Phi = -\frac{Gm}{\sqrt{d^2 + \epsilon^2}}, \quad (2)$$

where d denotes the distance of a disc element to the planet and ϵ is the smoothing-length. In our simulations, we used $\epsilon = 0.5 R_H$, where R_H denotes the Hill radius.

2.2 Initial orbits

Three $10 M_{\oplus}$ planetary cores were placed into the disc and were initially evolved till they reached a stable configuration in a resonance. We used a planet trap (Masset 2002; Masset et al. 2006a; Morbidelli et al. 2008) to halt the orbital migration of the innermost core.

The planet trap was set as a steep and locally positive surface-density gradient in the disc inside the initial orbital location of the innermost core. It allows the system of three cores to acquire stable, separated and non-migrating orbits. The planet trap is a convenient way to mimic the situation in real radiative discs where the non-isothermal effects can change the direction of the type-I migration (Paardekooper & Mellema 2006; Kley et al. 2009). The migration in the inner part of a real radiative disc can be directed outwards, while it remains directed inwards in the outer disc. This establishes the existence of a critical radius where migration vanishes. The planetary cores migrating inwards will be collected near this radius as in the case of a planet trap (Lyra et al. 2010).

The planet trap location was set at $a = 3$ in case A and $a = 2$ in case B . The local and positive surface-density gradient required to form the planet trap was created by imposing a transition in the viscosity from 4ν to ν over $\Delta r = 1$ around the trap location (Masset et al. 2006a). The initial orbits of the three cores were chosen near the 5:4 resonant chain in case A (semimajor axes $a_1 = 3.07$, $a_2 = 3.62$ and $a_3 = 4.20$), and near the 3:2 resonant chain in case B

¹ We use `swift_symba7` that is capable of correctly handling the closely packed planetary systems (Levison et al. 2011).

(semimajor axes $a_1 = 2.1$, $a_2 = 2.77$ and $a_3 = 3.66$). The initial eccentricities were set to zero.

In a first step, we followed the evolution of disc and cores, and waited till the cores arranged themselves in a stable resonant configuration. In case A, the cores 3 and 2 ended up in the 6:5 resonance, and cores 2 and 1 in the 7:6 resonance. In case B, two cores reached a coorbital configuration (1:1 resonance) near the planet trap, and the third one ended up in the 6:5 resonance with the other two. The eccentricities remained small at this stage, $e \sim 0.01$ – 0.02 , due to the strong damping of gas, and the orbits remained nearly coplanar.

2.3 Mass growth

Once the resonant configuration was achieved, the mass of each core was increased from the initial value ($m(0) = 3 \times 10^{-5} M_{\odot}$) to one Jupiter mass ($m_J = 10^{-3} M_{\odot}$) as follows:

$$m(t) = m(0) + (m_J - m(0)) \sin^2 \left(\frac{\pi (t - t(0))}{2 \Delta t} \right), \quad (3)$$

where $t(0)$ was the time when the growth started, and Δt was the growth time interval. Different values of $t(0)$ were chosen for different planets, so that they grew in sequence. Sometimes, we let the innermost core grow first with the other two growing later. In other cases, we opted for growing the middle or outer core first (see Section 3).

We did not consider gas accretion within the Roche lobe. This is a delicate point which is not well understood yet and which goes beyond the purpose of this work.

The criterion for collision is that the distance between planets becomes equal or lower to one Jupiter radius.

The time-scales for the planetary growth that we adopt ($\Delta t = 10^3$, 3×10^3 and 4×10^3 ; see Table 1) are too short to be realistic. These time-scales are dictated by our current CPU power (using the parallel FARGO code and 30 CPUs, we compute 10–100 orbits in 1 h, depending on the disc parameters). Slower growth rates will be investigated in the future.

When a planet grows to Jupiter mass, it is expected that the planet trap should become ineffective and the planet should start migrating inwards. We find this behaviour in our simulations.

3 DYNAMICS IN THE GAS DISC

Here, we discuss the orbital dynamics of growing planets in the full gas disc. Each system is evolved over 20 000–65 000 yr after the growth of the last planet. To identify the different settings of our simulations, we label them $A_{i,j,k}$ for case A and $B_{i,j,k}$ for case B, where indices $i, j, k \in [1, 3]$ indicate the growth order of the three cores (initially, $a_1 \leq a_2 < a_3$). The characteristics of each simulation are reported in Table 1.

Table 1. Simulations parameters.

Simulation	$[r_{\min}, r_{\max}]$	Δt	(N_r, N_s)
$A_{2,1,3}$	[0.5, 6.5]	10^3	(660,700)
$A_{3,1,2}$	[0.5, 9.5]	$\Delta t_3 = 4 \times 10^3$ $\Delta t_{1,2} = 10^3$	(660,700)
$A_{3,2,1}$	[1, 9.5]	3×10^3	(660,700)
	[0.5, 9.5] $t \geq 20\,000$		(700,700)
$B_{1,2,3}$	[0.5, 4.5]	10^3	(660,700)
	[0.1, 4.5] $t \geq 8500$		(720,700)
$B_{3,1,2}$	[0.5, 4.5]	10^3	(660,700)
	[0.1, 4.5] $t \geq 8500$		(720,700)
	[0.3, 4.5] $t \geq 30\,000$		(690,700)

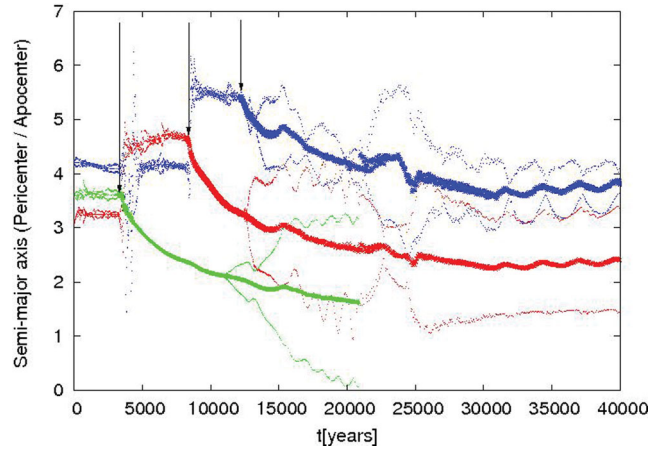


Figure 1. Dynamical evolution of the planets in simulation $A_{2,1,3}$. Each planet is represented by a different colour: red for planet 1 (initially the innermost one); green for planet 2 (middle); blue for planet 3 (outermost). For each planet, the three curves denote the pericentre, semimajor axis and apocentre as a function of time. The masses of the cores grow to Jupiter mass according to equation (3) on $\Delta t = 1000$ starting at $t_2(0) = 3200$, $t_1(0) = 8000$ and $t_3(0) = 12\,000$. The arrows highlight $t(0)$ for each planet.

3.1 Case $A_{2,1,3}$

Fig. 1 shows the results of simulation $A_{2,1,3}$. We find that when core 2 grows to Jupiter mass, it starts migrating inwards and scatters the other two cores at $a > 3$. We remark that the initial location of the trap is at $a = 3$, but the gap opened by core 2 has shifted the trap at $a = 4$. Therefore, cores 1 and 3 remain trapped at quasi-constant semimajor axis, respectively, at $a \simeq 4$ and $a \simeq 5.6$ till core 1 grows. As the fully grown planet 1 starts migrating inwards at $t = 8000$, it opens a gap and shifts the trap location at $a \simeq 5.5$. Core 3 is scattered out and remains near the new trap position at $a \simeq 5.5$ till $t_3(0) = 12\,000$. Core 3 then starts growing and inward migration begins.

Once all three planets reach Jupiter mass they migrate inwards and evolve into mutual resonances. Their orbital eccentricities rapidly grow to large values by resonant interactions. The system becomes highly unstable. The gas density distribution is strongly perturbed at this point (Fig. 2) leading to complex gas–planet interactions. Finally, at $t = 20\,000$ yr, the inner planet is lost by plunging into the star.

Our criterion for collision with the star is that the pericentre of the planet’s orbit becomes smaller than 0.01. The tidal effects are ignored in our simulation. In reality, however, the tidal effects should start to be dominant for small pericentres, potentially leading to the circularization of the orbit in the hot Jupiter region (Beauge & Nesvorný 2013). This effect would result in decoupling the planet from the other two. So, in any case, the inner planet’s influence on the other two is suppressed. The subsequent evolution of the two-planet system leads to stable orbits with moderate eccentricities.

3.2 Case $A_{3,1,2}$

In our first simulation, core 3 was grown on $\Delta t = 10^3$. One of the two remaining cores was ejected from the system during the growth of core 3. We have therefore reconsidered this case with a longer phase of growth of core 3, $\Delta t_3 = 4 \times 10^3$ (Table 1). In this case, the transition is less violent, core 2 is scattered out and its semimajor axis remains stable at the new trap location (after gap opening by planet 3), i.e. at $a \simeq 4.3$. Core 1 migrates inwards at the same rate

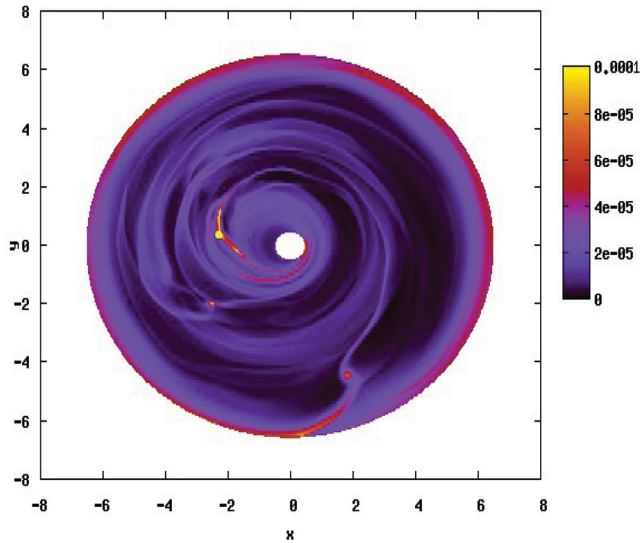


Figure 2. Gas surface density in the simulation shown in Fig. 1 at $t = 15\,000$. Three eccentric Jupiter-mass planets produce a complex distribution of gas. Colour scale range was chosen such that dark blue corresponds to values $\leq 10^{-5}$ and yellow to values $\geq 10^{-4}$ (in dimensionless units).

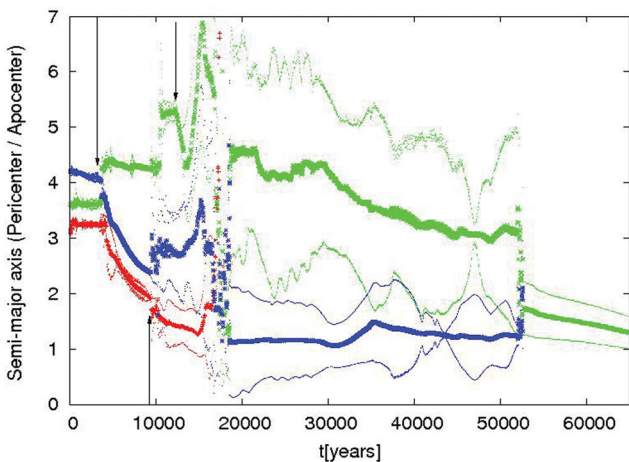


Figure 3. The same as Fig. 1 for the case $A_{3,1,2}$. The arrows highlight the $t_i(0)$ values: $t_3(0) = 3200$, $t_1(0) = 8700$ and $t_2(0) = 12\,000$.

as the fully grown planet 3 (Fig. 3). The growth of core 1 then leads to a phase when the other two planets are scattered outwards. The subsequent dynamics is complex with episodes of outward migration, and a rapid increase of the eccentricities after the growth of planet 2. As in case $A_{2,1,3}$, the system becomes highly unstable. Planet 1 is then ejected from the system. These early ejections could be related to free-floating planets (Sumi et al. 2011).

The orbits of the remaining two planets are chaotic till $t = 52\,594$, when the two planets merge.² The remaining giant planets migrates inwards and converges to a circular orbit.

3.3 Case $A_{3,2,1}$

In case $A_{3,2,1}$, all the three cores grow on $\Delta t = 3 \times 10^3$ (Fig. 4). The growth phase leads to the inward migration of the growing planet 3. The other two cores are scattered outwards. The subsequent phase is

² Note that merging events may happen too often in our simulations due to the coplanar approximation of the system.

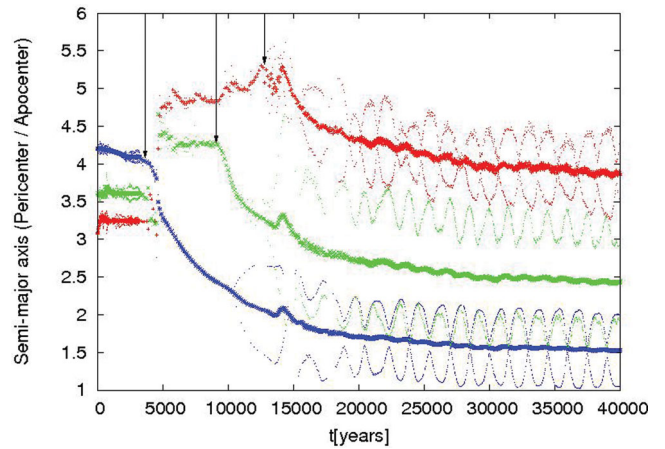


Figure 4. The same as Fig. 1 for the case $A_{3,2,1}$. The growth of cores started at $t_3(0) = 3200$, $t_2(0) = 8600$ and $t_1(0) = 12\,000$, as indicated by the arrows.

quite different with respect to the two previous cases. Here, the system settles in a stable resonant 2:1 configuration with planets slowly migrating inwards, and eccentricities reaching moderate values ($e \sim 0.2-0.3$).

We remark that three of the four planets found around the red dwarf Gliese 876 are on the triple 2:1 resonant configuration (Rivera et al. 2010). The masses of the planets as well as their distance from the star are different from our simulation so that our comparison is only qualitative but nevertheless interesting.

To avoid spurious boundary effects, the disc was extended to $r_{\min} = 0.5$ at $t = 20\,000$, when the pericentre of planet 3 was close to 1. The radial density profile has been extrapolated from the inner disc edge, and the simulation restarted with the extended disc.

3.4 Case $B_{1,2,3}$

In this case, cores 1 and 2 become coorbital at the trap location. It is interesting that they remain coorbital during the growth phase even if they do not grow at the same time (see Fig. 5). The third core is scattered out when planet 1 grows. It then migrates inwards until it reaches the trap at $a \simeq 2$. When its mass starts increasing, 3 migrates inwards, and all three planets reach in a compact orbital configuration. The disc has been extended to $r_{\min} = 0.1$ at $t = 8500$

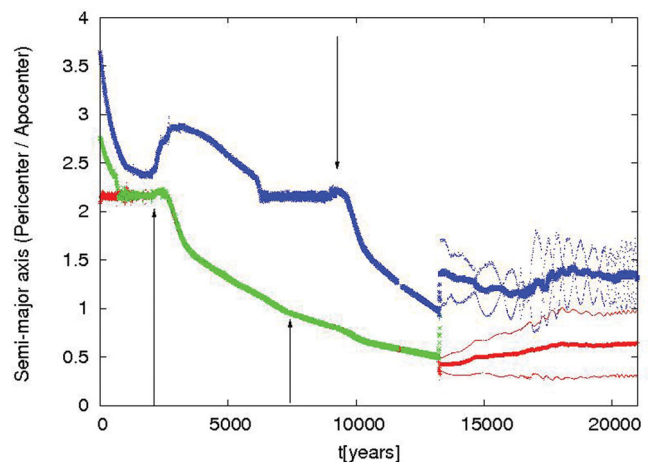


Figure 5. The same as Fig. 1 for the case $B_{1,2,3}$. The growth of cores started at $t_1(0) = 2000$, $t_2(0) = 7000$ and $t_3(0) = 9000$, as indicated by the arrows.

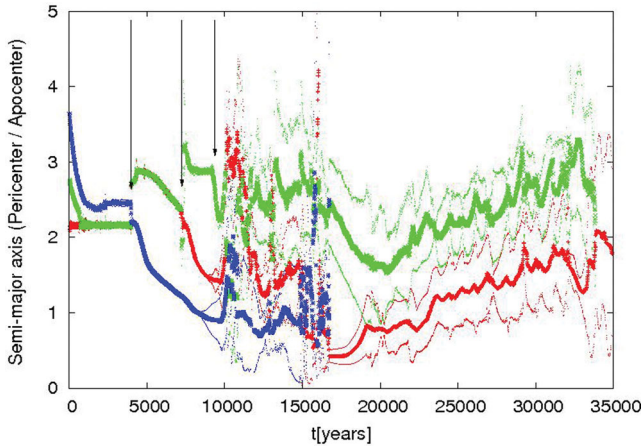


Figure 6. The same as Fig. 1 for the case $B_{3,1,2}$. The growth of cores started at $t_3(0) = 3700$, $t_1(0) = 7000$ and $t_2(0) = 9000$, as indicated by the arrows.

using the same procedure as for the case $A_{3,2,1}$. The extended disc is followed with a time-step of $\simeq 10^{-3}$. To calculate 10 orbits this requires about 1 h on 30 CPUs. The two coorbital planets merge at $t = 13\,275$ and the third one is scattered out. The eccentricities of the two remaining planets grow to moderate values. The planets end up in the 3:1 resonance.

3.5 Case $B_{3,1,2}$

Core 3 grows first and scatters two coorbital cores outwards. The two cores appear to be on the trap at very small angular separation $\Delta\alpha$ with: $10^\circ < \Delta\alpha < 30^\circ$. It is therefore possible that the scattering event affect them in the same way. Actually, as a result of the scattering they remain coorbital and only their angular separation changes drastically. The two orbits separate at $t = 7000$ when core 1 starts growing. Once that happens, core 1 scatters core 2 outwards (Fig. 6). After the growth of core 2, a complex instability arises resulting in the ejection of #3 from the system. The two remaining planets have moderate eccentricities and persist on chaotic orbits showing an outward migration trend till $t = 33\,900$ when the two planets merge. This case is comparable to the case $A_{3,1,2}$.

The disc has been extended to $r_{\min} = 0.1$ at $t = 8500$. In order to follow the chaotic evolution of the two planets on reasonable CPU times, we have then reduced the disc domain increasing r_{\min} to 0.3 at $t = 30\,000$.

3.6 Summary

From the limited number of cases that we have investigated so far, we can derive the following tentative implications for the dynamics of systems with three giant planets and their interaction with a gas disc:

(i) If the gas lasts long enough after the growth of the last giant planet, the system develops an instability and one planet is typically lost. These ejections could be related to free-floating planets (Sumi et al. 2011).

Indeed, only in one case out of five, we obtained a final stable system with three giant planets. This is at odds with the results of Matsumura et al. (2010) who found that the three-planet systems often survive to the end of gas disc lifetime. This difference may appear from the approximate treatment of the gas disc in Matsumura et al. (2010). When the gas density is strongly perturbed as in

Fig. 2, it acts as an additional source of stochasticity in the planetary evolution. Marzari et al. (2010), who used a hydrodynamical code similar to ours, also found that systems of fully grown giant planets on close orbits *rarely* survive to the end gas disc lifetime.

(ii) The simplified two-planet systems, which emerge from the three-planet systems when the third planet is eliminated, tend to be stabilized by their interaction with the gas disc. This was also pointed out in Marzari et al. (2010) and Matsumura et al. (2010), and in Moeckel, Raymond & Armitage (2008). In some cases, the two-planet system shows chaotic evolution till the system is reduced by a merging event. Future work on the full spatial problem will be needed to better explore the frequency of merging events.

(iii) We did not find any case where the giant planets would end up on nearly circular closely packed orbits. This raises doubts about the applicability of the initial conditions used in the models of planet scattering after the gas disc dispersal (see Section 1; Chatterjee et al. 2008; Juric & Tremaine 2008; Raymond et al. 2009).

4 GAS DISPERSAL AND GAS-FREE DYNAMICS

In the previous section, we assumed that the gas disc remains present after the accretion of the giant planets, that is, until the planets reach a stable dynamical configuration. It is possible, however, that the gas dispersal occurred *during* the planetary instability or soon after it, such that the planetary system did not have enough time to fully stabilize. Here, we investigate these cases.

The gas density was reduced at each time step dt as

$$\rho' = \rho \left(1 - \frac{dt}{\tau} \right), \quad (4)$$

where the coefficient $\tau \simeq 2000$ yr. This dissipation time-scale is very short when compared to the 10^5 yr time-scale considered for photoevaporation in Matsumura et al. (2010). We find that, if the gas is removed too fast, planetary systems can become unstable. In our simulations, we did not observe any scattering events or merging during the dissipation phase, so that we are confident that our results would not change much using a longer dissipation time-scale.

We recall that our purpose is not to quantitatively describe a specific phase of the giant planet–disc interaction but to obtain a qualitative description of the whole phenomenon; this justifies also the use of a dissipation function (4) which is simple with respect to the description in Moeckel & Armitage (2012).

When the disc gas density drops to values below $\sim 10^{-10}$ (in dimensionless units), the effect of gas becomes negligible and we continue the integration with SYMBA (Duncan et al. 1998). The planetary systems are evolved for up to 10^8 yr.

We first tried a case where gas was removed after the planetary system has reached its final configuration. Fig. 7 shows the orbits for the case $A_{2,1,3}$, where the gas disc was removed in the time interval [35 000, 37 000]. During the removal, planetary migration slows down and the two remaining planets stay in the 2:1 resonance for the whole N -body integration. The same applies to $B_{1,2,3}$, where no scattering event was found after the gas dispersal (gas was removed at [19 000, 20 000] in this case).

In $A_{3,2,1}$, where three planets initially survived, they also survived for the whole length of the N -body integration. The three planets remained in the 2:1 resonant chain and no scattering among them occurred (Fig. 8). This happened independently of the removal time (if chosen after $t = 20\,000$ yr in Fig. 4) and independently of the removal time-scale τ .

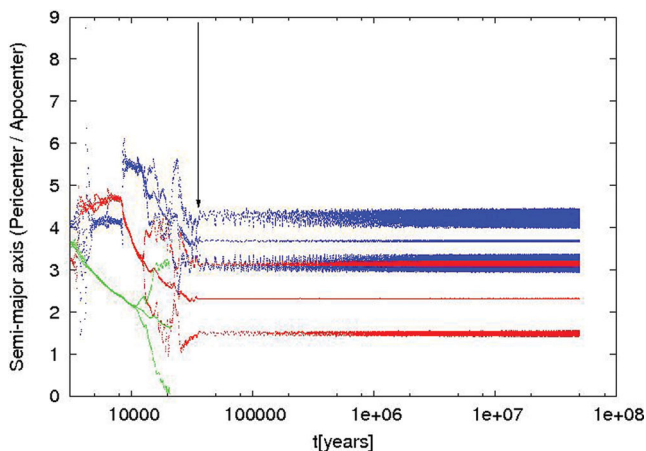


Figure 7. Evolution of planetary orbits in case $A_{2,1,3}$. The gas disc is removed at [35 000, 37 000], and an N -body integrator is used to follow the gravitational interactions among planets for $t > 37 000$. The arrow indicates the beginning of the gas-free phase.

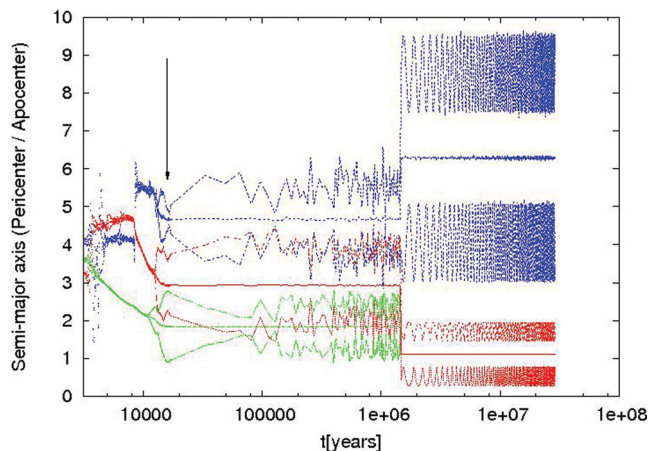


Figure 9. Evolution of planetary orbits in case $A_{2,1,3}$. The gas disc is removed at [15 000, 17 000]. The arrow indicates the beginning of the gas-free phase.

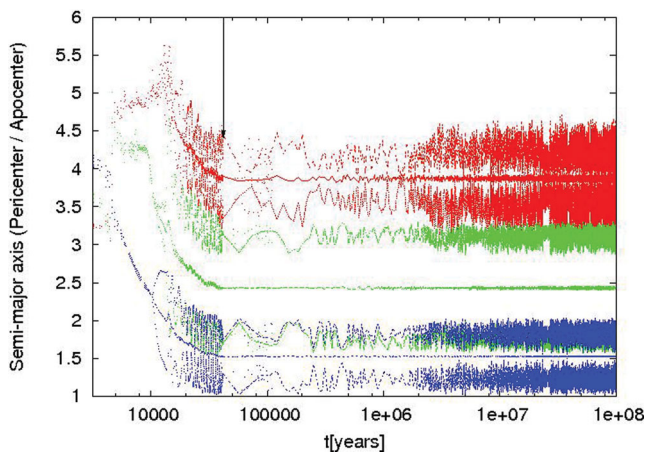


Figure 8. Evolution of planetary orbits in case $A_{3,2,1}$. The gas disc is removed at [39 500, 41 000]. The arrow indicates the beginning of the gas-free phase.

In Matsumura et al. (2010), in agreement with our results, the two-planet systems also remained stable. For the three-planet systems, Matsumura et al. (2010) found stability (e.g., see their fig. 4) only in some cases. Unfortunately, having only one three-planet system we cannot test the statistical significance of our result. Note also that the previous versions of the SYMBA code used in Matsumura et al. (2010) had a later-identified problem when tracking closely packed planetary systems (Levison et al. 2011). It has to be verified that this problem did not cause artificial instabilities in some of their integrations.

We now turn our attention to the possibility that the gas disc dispersed during the planetary-scattering phase. In Fig. 9, we removed gas in the interval [15 000, 17 000] during the evolution of system $A_{2,1,3}$ (Fig. 1). In this case, the three giant planets undergo a gravitational scattering event in which one planet is ejected and the remaining two are sent on to highly eccentric mutually decoupled orbits (Fig. 9). The same kind of evolution happened in all cases investigated here, provided that the gas disc was removed during the scattering phase.

5 CONCLUSIONS

We used a hydrodynamical code to follow the orbital evolution of systems of three planets as they grew in sequence to Jupiter mass. We found that the planet system changes drastically after the growth of each core. The orbital evolution of planets can be very complex. More often than not the orbits become unstable leading to a phase of planetary scattering. Planets can be ejected or merge (Marzari et al. 2010).

Once the system is reduced to two planets the dissipative effects of gas decrease orbital eccentricities of the remaining planets, and migrate planets into a new, stable resonant configuration. In only one case out of five, there was no instability happening after the growth of all three planets. The three-planet system remained in a resonant stable configuration in this case.

If the gas disc is removed after the new stable configuration is achieved, the orbital eccentricities remain low and the system is stable. This is at odds with the assumption typically made in the planet-scattering models (Chatterjee et al. 2008; Juric & Tremaine 2008; Raymond et al. 2009), where gas is ignored and the planets are initially placed on closely packed unstable orbits. Here, we show that these initial conditions may not naturally arise from a previous stage, in which the planets interacted with their natal protoplanetary disc.

If the gas disc is removed during the planetary instability, planetary scattering continues after the gas removal and the surviving planets can reach very eccentric orbits. However, given the short duration of the planetary instability phase, the removal of gas during this phase would require special timing. For example, it may be possible that the giant planets generally form towards the end of the disc lifetime. Or, as long as there is gas in the system, the existing giant planets keep growing and new giant planets keep forming. This would lead to a richer sequence of planetary instabilities than the one investigated here. We will investigate this possibility in the future work.

Another possibility is that the number of giant planets that form in a typical disc is large (>3). The N -body simulations have already shown that the eccentricity distribution of exoplanets implies that at least three giant planet existed in a typical system after the gas disc dispersal. Our results seem to suggest that, for this condition to be fulfilled, more than three planets have to form originally.

Alternatively, the giant planet systems that emerge from gas discs are stable in isolation, as suggested by in the simulations performed in this work, but become unstable due to external causes (interactions with smaller planets, effects of the planetesimal discs, etc.; e.g. Tsiganis et al. 2005; Levison et al. 2011).

In conclusion, the results presented here show that the problem of understanding the dynamical paths leading to the surprisingly large eccentricities of extrasolar planets is not fully resolved. Future work should improve upon our efforts by using more realistic prescriptions for the planet growth and gas dispersal, extend the simulation to longer time-scales and perform a larger number of simulations so that the statistical significance of individual outcomes and their dependence on disc parameters is better understood.

ACKNOWLEDGEMENTS

The computations have been done on the ‘Mesocentre SIGAMM’ machine, hosted by the Observatoire de la Côte d’Azur. DN acknowledges support from the NSF AAG programme.

REFERENCES

- Beaugé C., Nesvorný D., 2013, *ApJ*, 763, 12
 Chatterjee S., Ford E. B., Matsumura S., Rasio F. A., 2008, *ApJ*, 658, 580
 Duncan M. J., Levison H. F., Lee M. H., 1998, *AJ*, 116, 2067
 Holman M., Touma J., Tremaine S., 1997, *Nat*, 386, 254
 Juric M., Tremaine S., 2008, *ApJ*, 686, 603
 Kley W., Bitsch B., Klahr H., 2009, *A&A*, 506, 971
 Kokubo E., Ida S., 1998, *Icarus*, 131, 171
 Lee M. H., Peale S. J., 2002, *ApJ*, 567, 596
 Levison H. F., Morbidelli A., Tsiganis K., Nesvorný D., Gomes R., 2011, *AJ*, 142, 152
 Lin D. N. C., Ida S., 1997, *ApJ*, 477, 781
 Lyra W., Paardekooper S.-J., Mac Low M.-M., 2010, *ApJ*, 715, L68
 Marzari F., Baruteau C., Scholl H., 2010, *A&A*, 514, L4
 Masset F. S., 2000, *A&AS*, 141, 165
 Masset F. S., 2002, *A&A*, 387, 605
 Masset F. S., Morbidelli A., Crida A., Ferreira J., 2006a, *ApJ*, 642, 478
 Masset F. S., D’Angelo G., Kley W., 2006b, *ApJ*, 652, 730
 Matsumura S., Thommes E. W., Chatterjee S., Rasio F., 2010, *ApJ*, 714, 194
 Maze T., Krymowski Y., Rosenfeld G., 1997, *ApJ*, 477, L103
 Moeckel N., Armitage P. J., 2012, *MNRAS*, 419, 366
 Moeckel N., Raymond S. N., Armitage P. J., 2008, *ApJ*, 688, 1361
 Morbidelli A., Nesvorný D., 2012, *A&A*, 546, A18
 Morbidelli A., Crida A., Masset F., Nelson R. P., 2008, *A&A*, 478, 929
 Namouni F., 2005, *AJ*, 130, 280
 Paardekooper S.-J., Mellema G., 2006, *A&A*, 459, L17
 Pollack J. B., Hubickyj O., Bodenheimer P., Lissauer J. J., Podolak M., Greenzweig Y., 1996, *Icarus*, 124, 62
 Rasio F. A., Ford E. B., 1996, *Sci*, 274, 954
 Raymond S. N., Barnes R., Veras D., Armitage P. J., Gorelick N., Greenberg R., 2009, *ApJ*, 696, L98
 Rivera E. J., Laughlin G., Butler R. P., Vogt S. S., Haghighipour N., Meschiari S., 2010, *ApJ*, 719, 890
 Sumi T. et al., 2011, *Nat*, 473, 349
 Tsiganis K., Gomes R., Morbidelli A., Levison H. F., 2005, *Nat*, 435, 459
 Ward W. R., 1997, *Icarus*, 126, 261
 Weidenshilling S. J., Marzari F., 1996, *Nat*, 346, 619

This paper has been typeset from a \TeX/L\TeX file prepared by the author.